# Novel multi-user-MEMS-processes-compatible single-layer out-of-plane electrothermal actuator

**Weider Tang**
**Mingching Wu**
**Weileun Fang**
National Tsing Hua University
Power Mechanical Engineering Department
Hsinchu 30043, Taiwan
E-mail: fang@pme.nthu.edu.tw

**Abstract.** Microactuators are regarded as a key component in the field of microelectromechanical systems (MEMS). According to the motion of the actuator, it can be classified as an out-of-plane type or an in-plane type. Most of the existing out-of-plane thermal actuators are multi-layer structures. In this study, a novel electrothermal single-layer out-of-plane actuator is presented. The characteristics of this device are stated as follows: (1) This actuator consists of only a single thin film layer, therefore, it can prevent delaminating after a long-term operation. (2) The fabrication process is multi-user MEMS processes (MUMPs)-compatible, and it has the potential to integrate with many different micromachined components. (3) As demonstrated by the experiment, this device can be operated at a relatively low voltage. For the thermal actuator with beam length 275 $\mu$m, its deflection amplitude can reach 3.196 $\mu$m when driven at 5 V dc, and 5.316 $\mu$m when driven at 8 V dc. This structure offers the potential for application in adaptive optics systems and other optical systems. It also provides an interface to cooperate with integrated circuits and various optical elements to construct an embedded-control optical system. 
[DOI: 10.1117/1.1564595]

Subject terms: MEMS; electrothermal actuators; MUMPs.

Paper 02042 received Sep. 30, 2002; revised manuscript received Jan. 21, 2003; accepted for publication Feb. 3, 2003.

## 1 Introduction

Microactuators are regarded as a key component in the field of MEMS. According to the motion of the actuator, it can be classified as an out-of-plane type[1] or an in-plane type.[2] Presently, various approaches, such as electrothermal, magnetic, electrostatic, and piezoelectric, have been successfully employed to drive these actuators. Among typical driving approaches, electrothermal actuators[3–6] have the advantages of low operation voltage. Moreover, the electrothermal actuator has the potential to integrate with many different micromachined components by common surface micromachining processes, such as multi-user MEMS processes (MUMPs). Therefore, the thermal actuators are extensively employed to drive various MEMS devices.

The most common multi-layer thermal actuators exploit the bimorph effect to generate the out-of-plane motion. The multi-layer actuator consists of at least two thin films, and the coefficients of thermal expansion of these materials are different. The increasing of temperature will cause these materials to expand to different extents and result in an out-of-plane deflection. However, these actuators experience a shear force at the interface of two different layers when actuated. Thus, the delamination of each material may occur especially after a long-term operation and the lifetime of the devices is reduced.[7] To prevent this problem, a signal-layer in-plane thermal actuator has been presented in Refs. 7 and 8, and a signal-layer out-of-plane actuator has been presented in Refs. 9 and 10 as well. In Ref. 10, Chen et al. presented a bulk micromachined out-of-plane actuator that has bi-directional motions, i.e., upward and downward. However, the applications of this single-layer thermal actuator are restricted by its fabrication processes. In this study, a novel single-layer out-of-plane electrothermal actuator fabricated through MUMPs-compatible processes is proposed and demonstrated. Moreover, the performance and characteristics of this design are characterized.

## 2 Design and Analysis

As illustrated in Fig. 1(a), the electrothermal actuator presented in this paper consists of four identical and parallel beams. These four beams are connected with two connecting beams at the ends and formed a signal-layer structure. The inner beams are designed to have a step nearby the connecting beams. Thus, the inner beams are located at a higher level than the outer beams, as indicated in Fig. 1(b). During actuation, the current passes through the actuator from anchor A via the outer beams to anchor B. Hence points a1 and a2, as illustrated in Fig. 1(a), have the same potential, and so do points b1 and b2. Therefore, the temperature of the outer beams will increase and lead to a thermal expansion causing a bending moment that applies on the steps of the inner beams. The steps of the inner beams act as pivots and allow an upward out-of-plane deflection to occur.

In order to increase the deflection amplitude of the actuator, various geometric dimensions need to be considered.

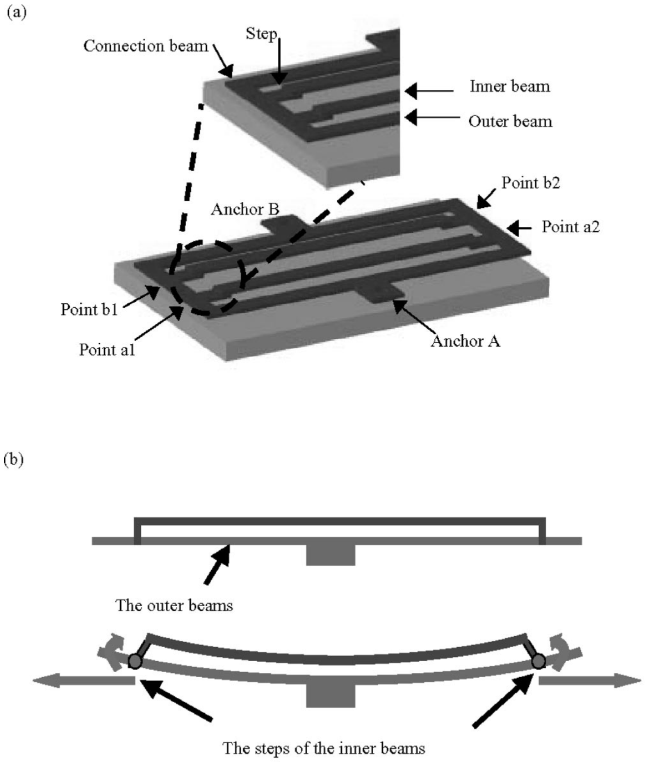


**Fig. 1** (a) The schematic drawing of the single-layer electrothermal actuator. (b) The illustration of the step design allows the outer beams to bend upward while the outer beams were heated.

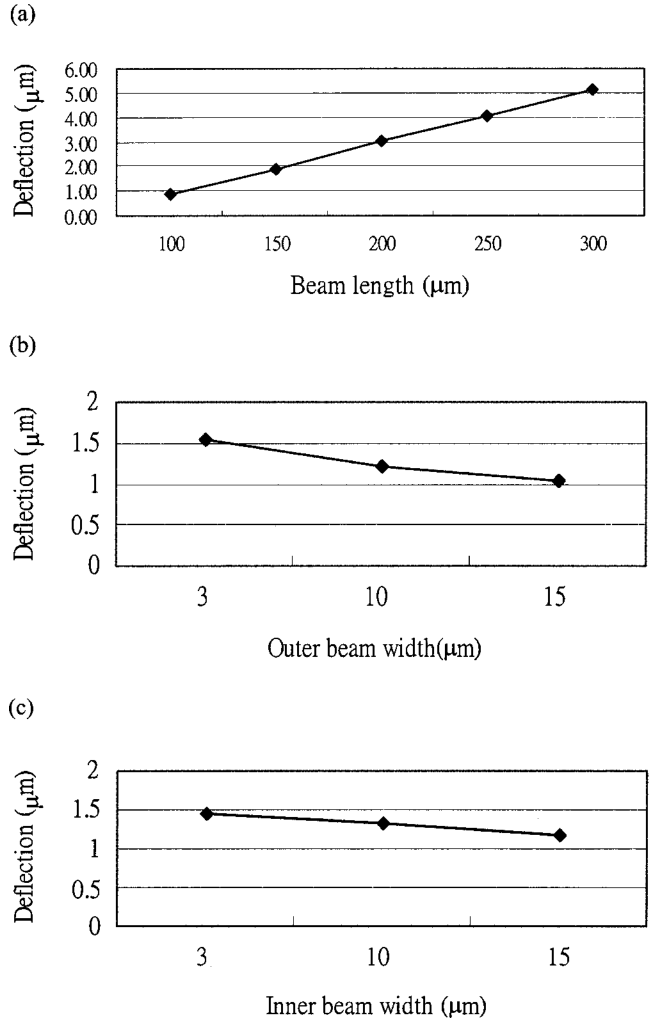


**Fig. 2** Geometric dimensions of the actuator: (a) deflection versus beam length, (b) deflection versus outer beam width, and (c) deflection versus inner beam width.

Because the beam thickness and the step height were determined by a common fabrication process, these two parameters were not taken into consideration. By means of finite element analysis software, only the beam length, outer beam width, and inner beam width are considered in the design. Figure 2 shows the simulation result of the thermal actuator with different geometric dimensions, and the conclusion is that the longer beam, narrower inner beam, and outer beam will lead to larger deflection amplitude. According to the simulation result, the geometric dimensions of the actuator are determined: the beam length is 275 $\mu$m from the anchor to the end of the beam, and the beam width is 3 $\mu$m for the inner and outer beam. The material properties used in the analysis are illustrated in Table 1.

Moreover, the characteristics of the actuator during operation have been studied through a simulation approach. A device with beam length of 275 $\mu$m (from the anchor to the end of the beam), outer beam width of 3 $\mu$m, and inner beam width of 3 $\mu$m is used as a typical study case. Figure 3 shows the simulation results of this actuator in terms of the upward deflection, temperature distribution, and current density. Figure 3(a) shows that the free ends of the actuator have the maximum deflection. These two free ends will be the output ends of the actuator. The temperature distribution of the thermal actuator is shown in Fig. 3(b). The finite element method (FEM) results show that the maximum temperature of the actuator is nearly 350 K. After carefully considering the heat transfer issue, the proposed design allows the temperature to be uniformly distributed over the whole actuator. Thus the breaking of the actuator due to overheating at a particular position can be prevented. Figure 3(c) shows that the current density in the inner beams is zero. In other words, the inner beams are not heating up by the electro-thermal effect. Apparently, the heat of the inner beams is conducted from the outer beams through the connecting arms. Figure 3(c) also demonstrates that the current of the proposed design only passes through the outer beams of the actuator, so as to allow the actuator to bend upward.

**Table 1** Polysilicon material properties used in the finite element analysis.

| Property | Polysilicon |
|---|---|
| Young's modulus | 1.65e5 |
| Coefficient of thermal expansion | 3.5e-6 |
| Thermal conductivity | 5.0e7 |
| Electric conductivity | 7.0e10 |
| Density | 2.23e-15 |

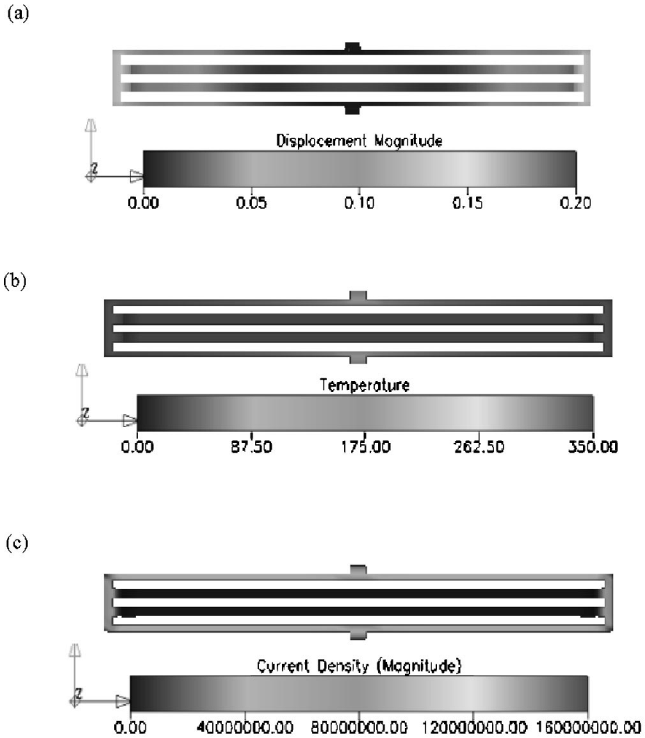


**Fig. 3** Simulation results of (a) upward deflection magnitude, (b) temperature, and (c) current density, for the driving voltage 3 V dc.

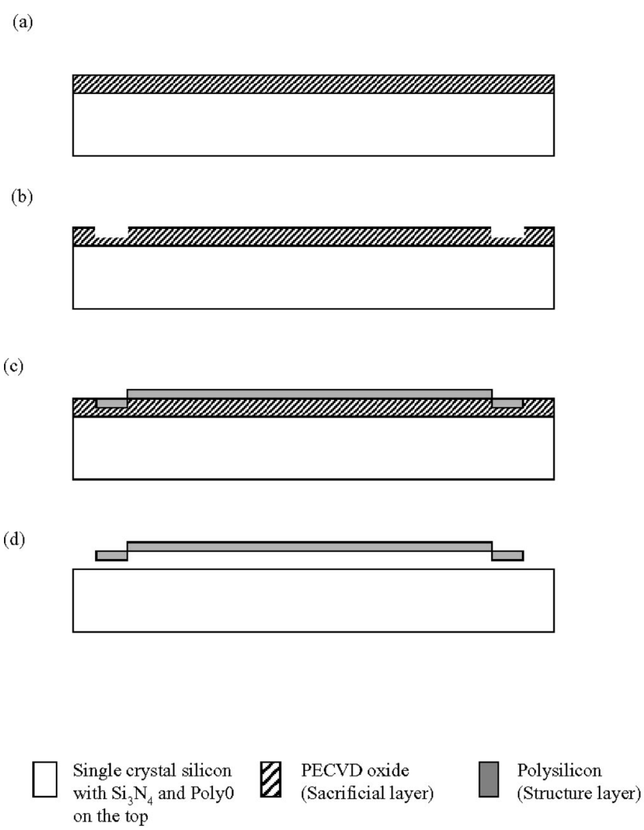


**Fig. 4** Fabrication processes of the proposed thermal actuator: (a) PECVD oxide deposition as the sacrificial layer, (b) pattern oxide to form dimple and anchor areas, (c) deposition LPCVD poly-Si as the structure layer, and (d) etching oxide to release the structure layer.

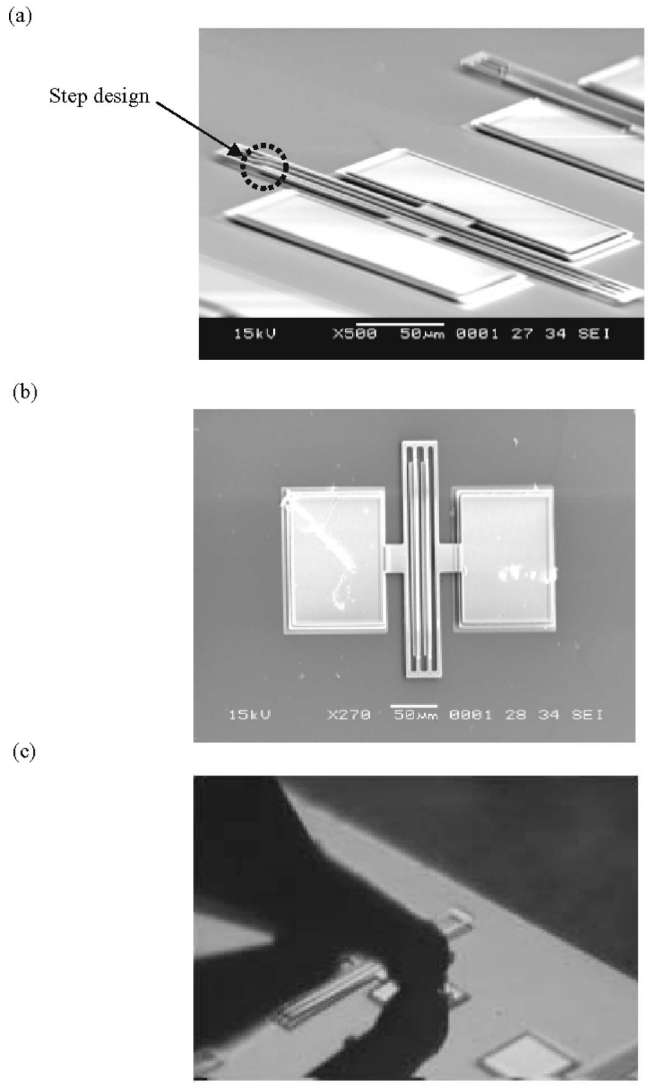


**Fig. 5** (a) The perspective view of the proposed thermal actuator, (b) the top view of the actuator, and (c) the actuated state of the actuator.

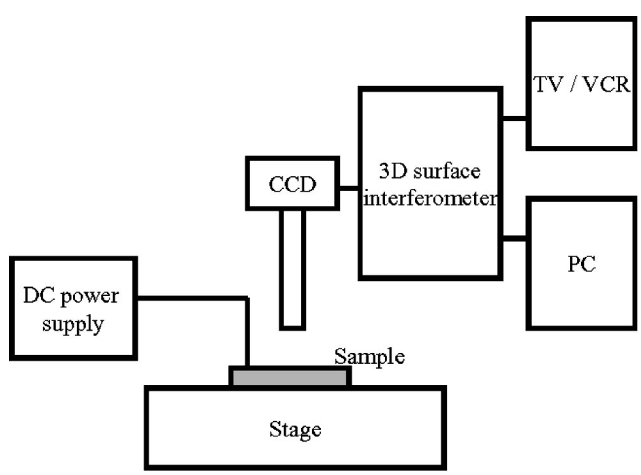


**Fig. 6** The experimental setup of the 3-D optical interferometer.

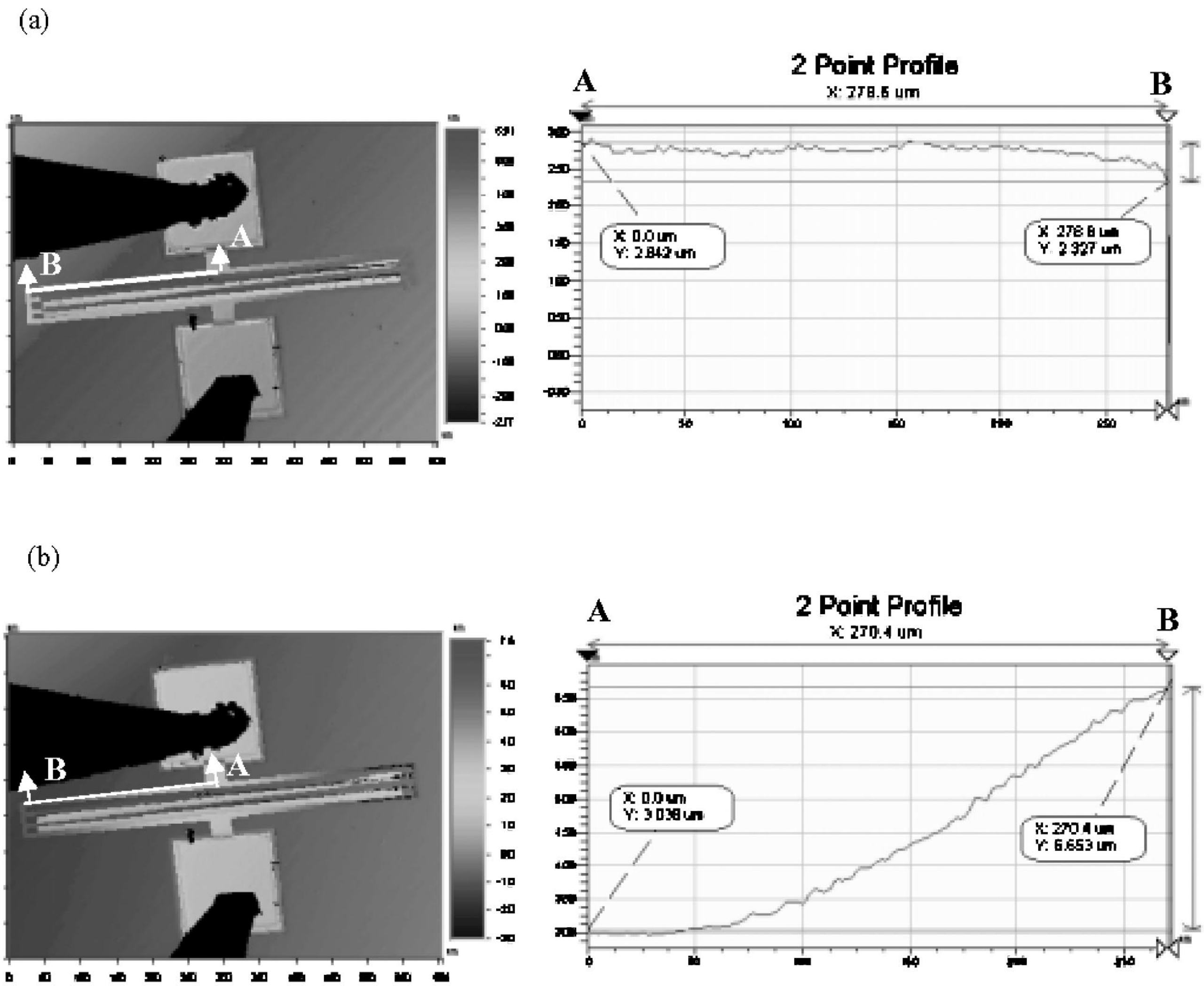


**Fig. 7** The static deflection of the actuator measured by the interferometer (a) when the driving voltage was 0 V dc and (b) when the driving voltage was 6 V dc.

## 3 Experiments

In order to demonstrate the concept of the proposed actuator, the actuator is fabricated and tested. Here, a modified MUMPs process[11] is employed in the fabrication. The three-photomask fabrication process is illustrated in Fig. 4. As shown in Fig. 4(a), the 0.5-$\mu$m-thick low pressure chemical vapor deposition (LPCVD) low-stress nitride film is deposited as the electrical isolation layer. After the first LPCVD polysilicon (poly0) layer of 0.5-$\mu$m thickness is deposited as the ground layer for electrical interconnections, the second low-stress nitride of 0.5-$\mu$m thickness is deposited as the electrical isolation layer again. A 2-$\mu$m-thick plasma enhanced chemical vapor deposition (PECVD) oxide is then deposited onto the surface of the silicon substrate to form the sacrificial layer. As shown in Fig. 4(b), these steps are followed by two photolithography processes to define dimple and anchor areas, respectively. In Fig. 4(c), the 2-$\mu$m-thick LPCVD polysilicon was deposited onto the sacrificial layer as the structure layer. The third mask is then used to define the geometric shape of the structure layer. Finally, in Fig. 4(d), the sacrificial layer is removed by hydrofluoric acid (HF) (49%) to release the structure. The scanning electronic microscope (SEM) pictures of the fabrication results are shown in Figs. 5(a) and 5(b). The step design is indicated in Fig. 5(a). The photo in Fig. 5(c) was taken during the driving test of the actuator. It is clearly observed that the two ends of the actuator are bent upward.

The experiment setup for measuring the upward deflection amplitude is illustrated in Fig. 6. First, the sample is put on the stage that can be translated along the x/y axis and tilted about the x/y axis as well. After the sample was well positioned, it was actuated by the dc power supply and inspected by the 3-D optical surface interferometer. Through the CCD attached to the interferometer, the deflection amplitude of the actuated device can be determined by the software. In addition, the image of the actuator can also be captured by the computer. A typical measured result for a 275-$\mu$m-long beam [from point A to point B indicated in Fig. 7(a)] is shown in Fig. 7. The measured surface topology of the actuator is represented by a different color. Figure 7(a) shows the measured deflection profile of the actua-

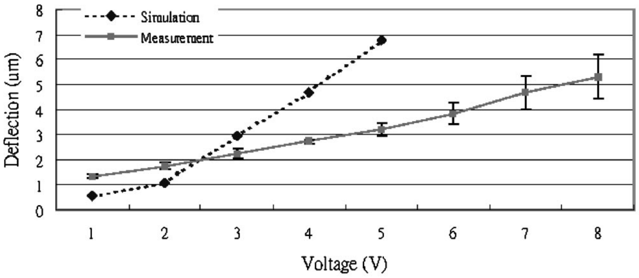


**Fig. 8** Variation of the deflection amplitude of the actuator with the driving voltage from 1 to 8 V dc.

tor along AB before actuation. Thus, the deflection profile of the actuator was mainly induced by the residual stresses of the thin film. The deflection amplitude of the actuator was 0.516 $\mu$m downward when driven with 0 V dc. As indicated in Fig. 7(b), the deflection profile of the actuator along AB was caused by the thermal effect during actuation. The deflection amplitude of the actuator was 3.614 $\mu$m upward when driven with 6 V dc. Consequently, the net deflection amplitude due to the thermal effect when driven with 6 V dc was 4.13 $\mu$m. The variation of the deflection amplitude and the driving voltage for a 275-$\mu$m-long beam is also shown in Fig. 8. The error bar in Fig. 8 represents the standard deviation of five different measurements.

## 4 Discussion and Conclusion

In Fig. 8, there are some deviations between the measured and simulated results, although their trends are matched. There are many reasons for this, and the major one is the contact resistance between the probe tip and the contact pad during measurement. Thus the actual driving voltage is smaller than the readout of the instrument, and the measured deflection is smaller than the simulated results. Wire bonding could further improve this problem instead of using a probe in the measurement. Another error source may come from the instability of the fabrication processes.

A novel single-layer out-of-plane thermal actuator has been designed and fabricated. The thermal actuator was fabricated by modified MUMPs processes. Since the fabrication processes are compatible with MUMPs, the proposed thermal actuator has the potential to integrate with various existing passive surface micromachined structures. According to the measurement, the deflection amplitude of the presented 275-$\mu$m-long thermal actuator can reach 3.196 $\mu$m when driven at 5 V dc, and 5.316 $\mu$m when driven at 8 V dc. Because the proposed thermal actuator consists of only one thin film material, it can prevent delamination and the lifetime of this device is significantly improved.

### *Acknowledgments*

The authors would like to express their appreciation to the NSC Central Regional MEMS Research Center (Taiwan), Electrical Engineering Department of National Tsing Hua University (Taiwan), Semiconductor Center of National Chiao Tung University (Taiwan), and National Nano Device Laboratories (Taiwan) in providing fabrication facilities.

### *References*

1. H.-Y. Lin and W. Fang, ''Out-of-plane comb drive lever actuator,'' *Proc. 2000 ASME IMECE*, Orlando, FL, pp. 97–104 (Nov. 2000).
2. W. C. Tang, T-C. H. Nguyen, and R. T. Howe, ''Laterally driven polysilicon resonant microstructures,'' *1989 IEEE MEMS Conf.*, Salt Lake City, UT, pp. 53–59 (Feb. 1989).
3. S. Schweizer, S. Calmes, M. Laudon, and P. Pemaud, ''Thermal actuated optical microscanner with large angle and low consumption,'' *Sens. Actuators A* **76**, 470–477 (1999).
4. X.-Q. Sun, K. R. Farmer, and W. N. Carr, ''A bistable microrelay based on two-segment multimorph cantilever actuators,'' *Proc. IEEE MEMS'98*, Heidelberg, Germany, pp. 154–159 (Jan. 1998).
5. J. M. Noworolski, E. H. Klaassen, J. R. Logan, K. E. Petersen, E. Kurt, and N. I. Maluf, ''Process for in-plane and out-of-plane single-crystal-silicon thermal microactuators,'' *Sens. Actuators A* **55**, 65–69 (1996).
6. J. W. Suh, C. W. Storment, and G. T. A. Kovacs, ''Characterization of multi-segment organics thermal actuators,'' *Transducer '95*, Stockholm, Sweden, pp. 333–336 (June 1995).
7. J. H. Comtois and V. M. Bright, ''Applications for surfacemicromachined polysilicon thermal actuators and arrays,'' *Sens. Actuators A* **58**, 19–25 (1997).
8. D. M. Burns and V. M. Bright, ''Design and performance of a double hot arm polysilicon thermal actuator,'' in *Micromachining and Microfabrication*, *Proc. SPIE* **3224**, 296–306 (1997).
9. C. Lo, H.-Y. Lin, and W. Fang, ''A novel out-of-plane electrothermal microactuator,'' *2001 Microsystem Tech. Conf.*, Dusseldorf, Germany, pp. 223–229 (March 2001).
10. W. C. Chen, J. Hsieh, and W. Fang, ''A novel single-layer bidirectional out-of-plane electrothermal microactuator,'' *Fifteenth IEEE Internal Conf. on Micro Electro Mechanical Systems*, Las Vegas, Nevada, pp. 693–699 (2002).
11. Y.-P. Ho, Master's Thesis, National Tsing-Hua Univ, Taiwan (2002).

**Weider Tang** received his MS degree in power mechanical engineering (PME) from Tsing-Hua University, Hsinchu, Taiwan, in 2000. Currently he is working toward a doctoral degree in PME at Tsing-Hua University. His research is focused on micromachined structure design, microfabrication, and microactuator and micro-optical system design, and he is also interested in microscale science.

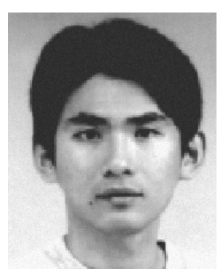

**Mingching Wu** received his MS degree in power mechanical engineering (PME) from Tsing-Hua University, Hsinchu, Taiwan, in 2001. He is currently a PhD student in PME at Tsing-Hua University and is researching the design and fabrication of micromachined devices.

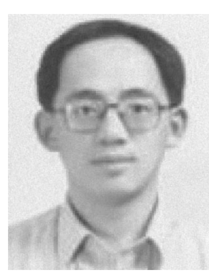

**Weileun Fang** received his PhD degree from Carnegie Mellon University in 1995. His doctoral research focused on determining the mechanical properties of thin films using micromachined structures. In 1995, he worked as a postdoctoral researcher at Synchrotron Radiation Research Center, Taiwan. He is currently an associate professor at Power Mechanical Engineering Department, National Tsing Hua University, Taiwan. His research interests include MEMS with an emphasis on micro-optical systems, microactuators, and the characterization of the mechanical properties of thin films.